UV Absorption Spectra of Intermediates Generated via Photolysis of $B(N_3)_3$, $BCl(N_3)_2$, and $BCl_2(N_3)$ in Low-Temperature Argon Matrices†

Michael J. Travers and Julanna V. Gilbert*

Department of Chemistry and Biochemistry, University of Denver, Denver, Colorado 80208

Received: November 5, 1999; In Final Form: January 31, 2000

The UV absorption spectra of $B(N_3)_3$, $BCl(N_3)_2$ and BCl_2N_3 isolated in low temperature argon matrices were measured as the matrices were photolyzed with the loosely focused output of a D_2 lamp. IR spectra were taken simultaneously with the UV spectra, and changes in the UV spectra were correlated with changes in the IR spectra. A series of bands at 348.0, 353.5, 360.0, 366.0, 372.5, and 379.5 nm appeared during the photolysis of $B(N_3)_3$ and were assigned as a vibrational progression in a bending mode of NNBN. Photolysis of $BCl(N_3)_2$ generated a feature at 408 nm that displayed evidence of vibrational structure and a sharp band at 275 nm. The 408 nm absorption was tentatively assigned to $ClBN_2$, a three-membered ring compound, and the 275 nm band as the $A^1\Pi \leftarrow X^1\Sigma$ transition in BCl. No new UV features were observed during the photolysis of BCl_2N_3, although the IR spectrum clearly indicated the formation of ClBNCl. These data indicate that ClBNCl has no UV absorption spectrum at wavelengths longer than 240 nm.

Introduction

The study of the processes by which energetic species react to form useful products has been of special interest in our laboratory, and our most recent work has centered around understanding the photolytic decomposition by which BN films are generated from $B(N_3)_3$. The formation of these films via the spontaneous decomposition of $B(N_3)_3$ was first reported by Coombe and co-workers, who also observed that the formation of the cubic form was enhanced upon UV irradiation.[1] A simple gas-phase synthesis of $B(N_3)_3$ via the reaction of 3 to 1 mixtures of HN_3 and BCl_3 was also reported by Coombe.

Using the technique of low-temperature matrix isolation, photolysis studies of $B(N_3)_3$ have been carried out, and the interesting intermediate NNBN was identified.[2] NNBN was also observed in a series of experiments done by the Andrews group in which laser ablation was used to produce boron atoms in a flow of nitrogen.[3] These studies imply that NNBN is an important intermediate in boron−nitrogen systems and may well be key for BN film formation.

The appearance of NNBN provides confirmation of the assumption that photolysis of $B(N_3)_3$ is similar to photolysis processes in other covalent azides, resulting in cleavage of the $RN-N_2$ bond of the azide groups and the release of molecular nitrogen. It also implies that an initially formed trigonal fragment BN_3 rearranges to the linear NNBN form. This can be envisioned as the two-step process shown in Figure 1A. To explore the possibility that this process is active in other boron azides, low-temperature matrix studies of the compounds BCl_2N_3 and $BCl(N_3)_2$ have also been performed.[4,5] The first of these, BCl_2N_3, had been previously synthesized via the reaction of ClN_3 and BCl_3 and isolated as a trimer.[6] In our lab, the monomeric form of BCl_2N_3 is synthesized with the same apparatus used to prepare $B(N_3)_3$ by simply adjusting the HN_3/BCl_3 reagent ratio to 1/1. The results obtained from our photolysis studies of BCl_2N_3 in a low-temperature argon matrix do indeed support the $B(N_3)_3$ mechanism. Upon photolysis, the linear molecule ClBNCl appeared, indicating that in the photolytic decomposition, the release of N_2 is followed by the rearrangement of the trigonal BCl_2N fragment, as is shown in Figure 1B. No previous reports of the second compound, $BCl(N_3)_2$, had appeared in the literature, but by adjusting the HN_3/BCl_3 ratio to 2/1 in the gas-phase synthesis apparatus, this compound was also synthesized and deposited in a low-temperature argon matrix. Photolysis of the $BCl(N_3)_2$/Ar matrix did not generate a linear intermediate, but rather evidence for the formation of a three-membered ring compound, $ClBN_2$, was obtained. Figure 1C shows the formation of this ring compound from the trigonal $BClN_2$, and again the release of N_2 is followed by rearrangement. This stable ring structure is a photolysis product for which no analogues were detected in the $B(N_3)$ and BCl_2N_3 systems.

The only spectral data available for the three intermediates identified (NNBN, ClBNCl, and $ClBN_2$) are their IR spectra. To fully characterize these molecules and to understand their behavior in a photolytic environment, information regarding their electronic states is needed. This paper reports the UV absorption spectra taken as a function of photolysis time of matrices containing the parent species $B(N_3)_3$, BCl_2N_3, and $BCl(N_3)_2$. Peaks appear in the UV that correlate with the IR features for NNBN and $ClBN_2$. For ClBNCl, no UV spectrum is observed.

Experimental Section

The experimental apparatus used in the following experiments has been described in detail elsewhere.[2] Briefly, the boron azide molecules are generated by the reaction of HN_3 and BCl_3, each diluted to 1% in argon. HN_3 is synthesized by reacting NaN_3 in excess stearic acid,[7] with the gaseous product collected and diluted in argon (99.999%). Hydrozoic acid is explosive and toxic and should be handled with extreme care. BCl_3 is purchased from Matheson and used without further purification.

The precursor gases are regulated using two Tylan 10 sccm flow meters equipped with metering needle valves and continu-

† Part of the special issue "Marilyn Jacox Festschrift".

10.1021/jp993939j CCC: $19.00
Published on Web 03/31/2000

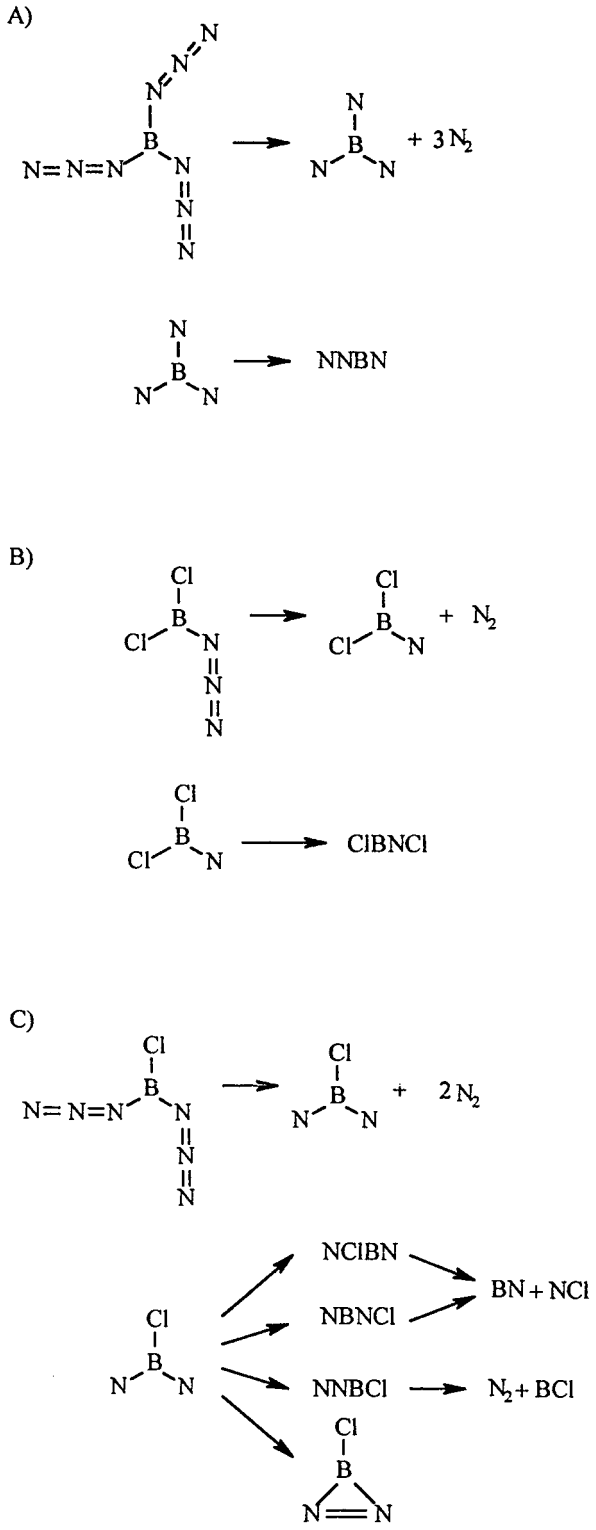

Figure 1. Photolysis schemes for (A) generation of NNBN from $B(N)_3$, (B) generation of ClBNCl from BCl_2N_3, and (C) generation of the ring compound $ClBN_2$, N_2 + BCl, and BN + NCl from $BCl(N_3)_2$.

ously flowed through a 5 L Pyrex reaction bulb such that the retention time in the flow system is typically 8 min for the conditions used in these experiments. The HN_3/BCl_3 flow ratio is adjusted to produce the desirable product, $B(N_3)_3$, $BCl(N_3)_2$, or BCl_2N_3. A small proportion of the effluent from the 5 L Pyrex bulb is admitted via a stainless steel metering valve into the cold head in which a 25 mm KCl deposition window is maintained at 10 K by a closed-cycle He cryostat (RMC model 22).

The cold head is positioned in the sample chamber of a Nicolet 5DXPC FTIR spectrometer (resolution 2 cm^{-1}) to monitor the deposition and photolysis processes in situ. A Spectral Instruments model 44-UV/vis spectrometer (resolution 1 nm) equipped with fiber optics and a CCD array detector is used to collect the UV absorption spectra. The fiber optic cables are positioned on either side of the cold head so that the UV beam passes through the deposition window at right angles to the IR beam. These fibers are equipped with optics so that a parallel UV light beam is passed through the sample, thereby greatly improving the throughput. The loosely focused, broad-band output of a D_2 lamp travels in the opposite direction of and slightly off axis to the UV absorption light beam to minimize the amount of the photolysis light that is admitted to the UV spectrometer detector. Mounted on the vacuum shroud of the cold head are two 50 mm KCl windows and two 50 mm UV-quartz windows for passing the IR light beam and the UV light beams, respectively. This arrangement allows the UV absorption and IR absorption spectra to be collected simultaneously as the matrices are photolyzed.

Results

Photolysis of $B(N_3)_3$. A low-temperature argon matrix containing $B(N_3)_3$ was prepared using the procedure reported in ref 2. Upon photolysis, the IR spectra showed the disappearance of the $B(N_3)_3$ parent peaks and the appearance of the NNBN product peaks, in agreement with our previously published data. Figure 2A shows a typical IR spectrum of NNBN produced in this way with the characteristic peaks at 1803, 1861, and (not shown) 2100 cm^{-1}. Figure 3 shows the UV difference spectra collected as a function of photolysis time. In these spectra, the spectrum collected just as the photolysis began is subtracted from each subsequent spectrum. A total of 20 spectra were recorded at 5 min intervals, and Figure 3 shows every other spectrum collected. The negative peak at 237 nm is assigned to the parent $B(N_3)_3$ and agrees well with the 230 nm value published for gas-phase $B(N_3)_3$.[1] The 237 nm feature becomes more negative as the photolysis proceeds, indicating its disappearance as new features at 254, 275, and 338 nm and a series of bands between 345 and 380 nm appear. The 275 nm feature is assigned as the $A^1\Pi \leftarrow X^1\Sigma$ absorption band of BCl slightly red shifted due to matrix affects,[8] and its source is discussed in the next section. The prominent 338 nm peak is assigned as the $A^3\Pi \leftarrow X^3\Sigma$ transition of NH,[8] formed via the photolysis of excess HN_3 deposited in the matrix. This feature is also observed when HN_3 only is deposited and photolyzed in an argon matrix.

UV and IR spectra were collected simultaneously during the photolysis so that the growth of known IR features could be compared to that of new UV features. A plot of normalized absorbance vs photolysis time is shown in Figure 4 for features from the IR and UV absorption spectra collected during the photolysis of the $B(N_3)_3$ matrix. The broad feature at 254 nm displays the fastest growth and the NH and BCl absorptions at 338 and 275 nm, respectively, the slowest growth as a function of photolysis time. It is noted, however, that because the 254 nm feature overlaps the $B(N_3)_3$ absorption, its growth behavior is distorted by the changing baseline. These data do not provide information that allows the assignment of the 254 nm, and this feature warrants further study. The growth of the series of peaks between 345 and 380 nm closely matches that of the NNBN infrared peaks at 1803 and 1861 cm^{-1}. Hence, this series of bands is assigned to NNBN. The IR normalized intensities are consistently slightly lower than are the UV-

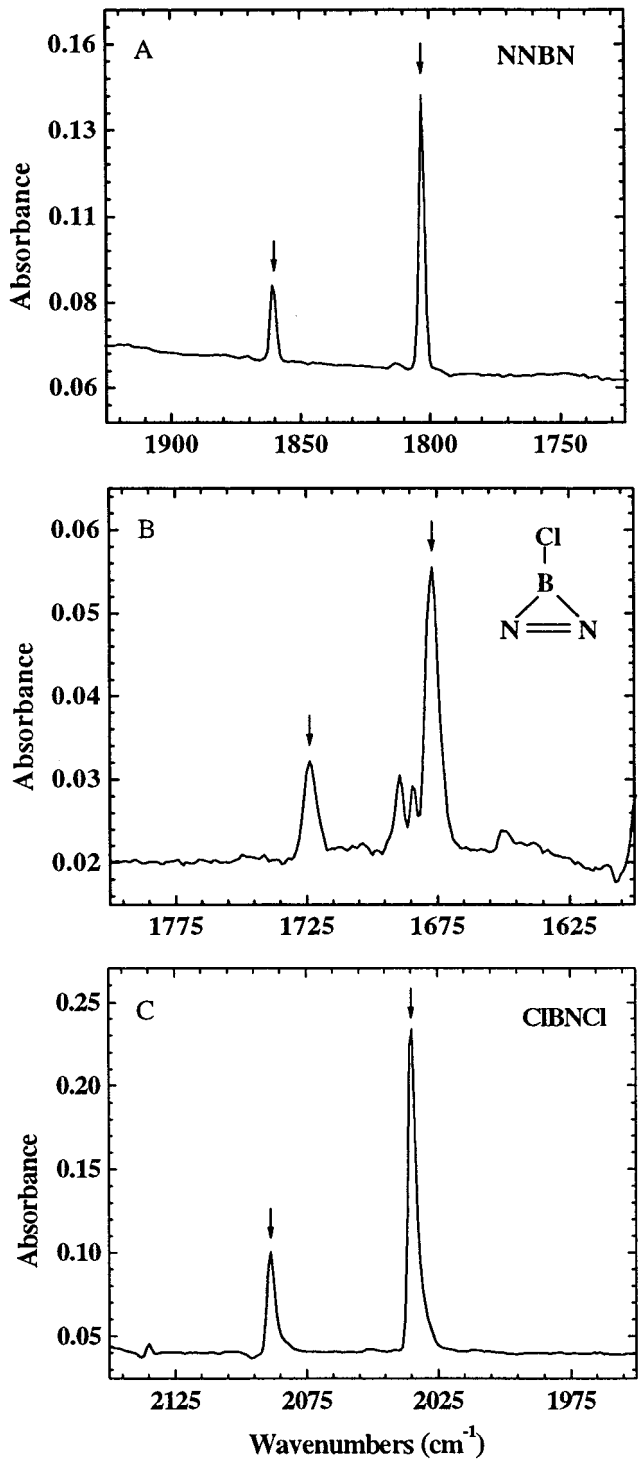

Figure 2. Infrared spectra of intermediates generated from the photolysis of the parent boron azides in low-temperature argon matrices: (A) NNBN from photolysis of $B(N_3)_3$, (B) $ClBN_2$ (tentative assignment) from photolysis of $BCl(N_3)_2$, and (C) ClBNCl from photolysis of BCl_2N_3.

normalized intensities, reflecting the fact that there was a constant, short lag time between the collection of the IR and UV spectra.

When the absorption scale of Figure 3 is expanded, a very weak feature at 408 nm appears. It is not possible to obtain reliable growth data for this peak because it is so weak, but its presence in this spectrum is noted for later reference.

Photolysis of $BCl(N_3)_2$. Although it is possible to prepare matrices in which the major boron azide species deposited is

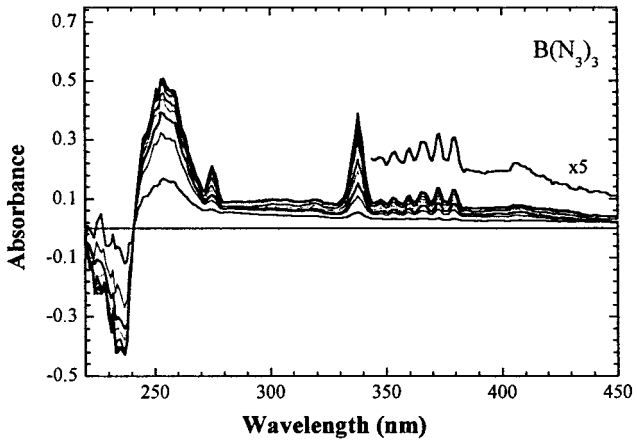

Figure 3. UV absorption spectra collected as a function of photolysis time of $B(N_3)_3$ in a low-temperature argon matrix. These are difference spectra in which the spectrum collected just as the photolysis began is subtracted from each successive spectrum. Features at 254, 275, and 338 nm appear as well as a series of bands between 345 and 380 nm. The negative feature at 237 nm shows the disappearance of the $B(N_3)_3$ parent. Spectra were collected at 5 min intervals, and every other spectrum is included in this figure, giving a 10 min interval for the spectra shown.

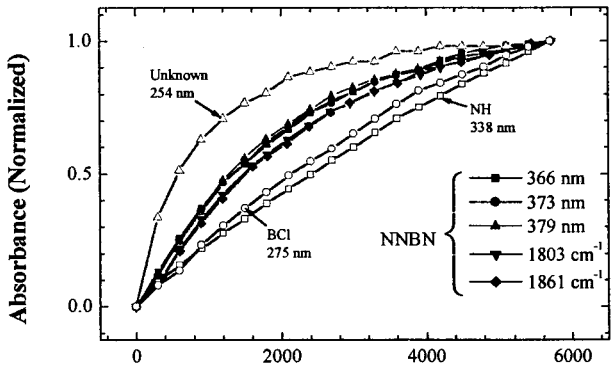

Figure 4. Plots of normalized absorbance vs photolysis time from the spectral data used in Figure 3 for the photolysis of $B(N_3)_3$. The UV bands between 345 and 380 nm grow at the same rate as the IR bands assigned to NNBN. Other features as indicated display different growth characteristics.

$BCl(N_3)_2$, there is always some BCl_2N_3 and/or $B(N_3)_3$ present as well in the matrix. For the photolysis studies, this is not a problem since a comparison of the experimental results from mixed matrices to those of nearly pure BCl_2N_3 or $B(N_3)_3$ matrices can be made. The infrared spectrum of the matrix chosen for this paper indicated that small amounts of BCl_2N_3 were deposited in the matrix along with the $BCl(N_3)_2$. Upon photolysis, IR peaks at 1677, 1724, 2034, and 2087 cm^{-1} appeared. The IR difference spectrum (Figure 2B) shows the 1677 and 1724 cm^{-1} bands that are tentatively assigned to ^{10}B and ^{11}B isotopomers of $ClBN_2$ based our previous photolysis study of $BCl(N_3)_2$.[5] The IR bands at 2034 and 2087 cm^{-1} are the ^{10}B and ^{11}B isotopomers of ClBNCl, generated from the photolysis of BCl_2N_3.[4]

The UV difference spectra collected during the photolysis are shown in Figure 5. The negative peak at 235 nm is due to the parent species ($BCl(N_3)_2$ and BCl_2N_3) and becomes more negative, indicating loss during photolysis. An intense band at 275 nm and a broad feature with a maximum at 408 nm appear. Both of these peaks were observed in the $B(N_3)_3$ data (Figure 3), suggesting the same source in both matrices. The 275 nm peak is the $A^1\Pi \leftarrow X^1\Sigma$ transition in BCl.

To assign the 408 nm peak, a comparison of the UV and IR

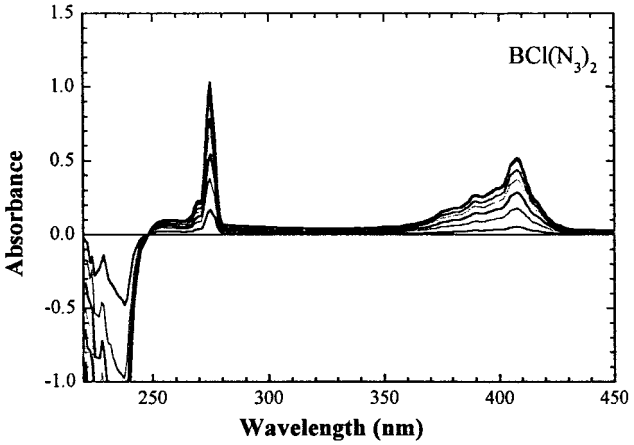

Figure 5. UV absorption spectra collected as a function of photolysis time of $BCl(N_3)_2$ in a low-temperature argon matrix. These are difference spectra in which the spectrum collected just as the photolysis began is subtracted from each successive spectrum. Features at 275 and 408 nm appear. The negative feature between 200 and 240 nm shows the disappearance of the parent species. Spectra were collected at 5 min intervals, and every other spectrum is included in this figure, giving a 10 min interval for the spectra shown.

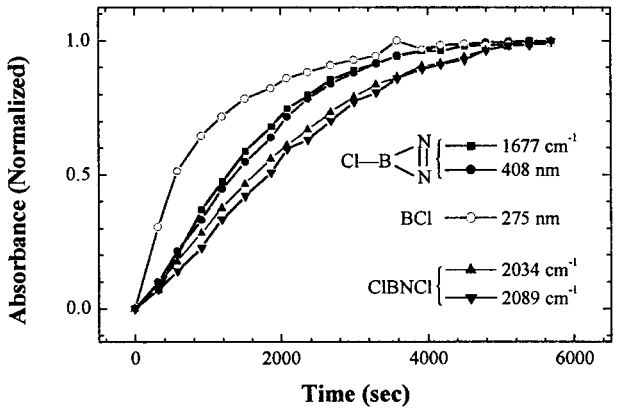

Figure 6. Plots of normalized absorbance vs photolysis time from the spectral data used in Figure 5 for the photolysis of $BCl(N_3)_2$. The UV band at 408 nm grows at the same rate as the IR bands tentatively assigned to the three-membered ring compound $ClBN_2$. This matrix also contained some BCl_2N_3, and the production of ClBNCl is from photolysis of this compound. The growth of the ClBNCl peaks is slower than that of the intermediate generated from $BCl(N_3)_2$. The 275 nm peak is due to BCl that is generated from photolysis as discussed in the text.

spectra as a function of photolysis time is made. Figure 6 shows the normalized absorbances for the 275 and 408 nm UV peaks and for the 1677, 2034, and 2089 cm^{-1} IR peaks plotted vs photolysis time. The 1677 cm^{-1} and the 408 nm features display the same growth behavior, whereas the ClBNCl peaks at 2034 and 2087 cm^{-1} grow in more slowly. To confirm the correlation between the 408 nm UV and the IR 1677 cm^{-1} features, the experiment was repeated several times. In two of the experiments the photolysis was continued for an extended period of time until virtually none of the parent azides remained in the matrix. In these cases, the 408 nm and 1677 cm^{-1} features were observed to decay whereas other features in the UV and IR spectra did not. On the basis of these photolysis characteristics, the 408 nm feature and the 1677 cm^{-1} features are assigned to the same species, assumed to be $ClBN_2$ (as discussed below). The 275 nm band, assigned to the $A^1\Pi \leftarrow X^1\Sigma$ transition in BCl grows in faster than any of the other features.

Photolysis of BCl_2N_3. When the HN_3/BCl_3 ratio is maintained at less than unity, matrices containing BCl_2N_3 are produced.

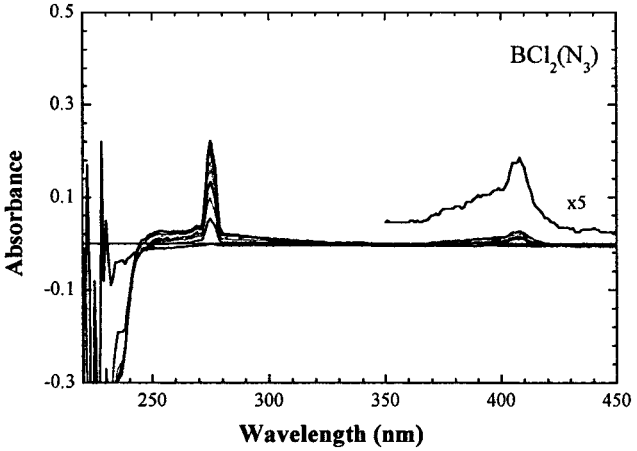

Figure 7. UV absorption spectra collected as a function of photolysis time of BCl_2N_3 in a low-temperature argon matrix. These are difference spectra in which the spectrum collected just as the photolysis began is subtracted from each successive spectrum. Features at 275 and 408 nm appear but are from photolysis of $BCl(N_3)_2$ that is also present in this matrix, as discussed in the text. The negative feature between 200 and 240 nm shows the disappearance of the parent species. Spectra were collected at 5 min intervals, and every other spectrum is included in this figure, giving a 10 min interval for the spectra shown.

Photolysis of this compound generates ClBNCl,[4] and its IR spectrum with features at 2034 and 2087 cm^{-1} is shown in Figure 2C. The IR spectrum of the matrix used for these studies indicated that a small amount of $BCl(N_3)_2$ was also deposited.

The UV spectra collected as a function of photolysis time are shown as difference spectra in Figure 7. These spectra look nearly identical to those obtained for the $BCl(N_3)_2$ matrix with the features appearing at 275 and 408 nm assigned to BCl and $ClBN_2$, respectively. Apparently, ClBNCl, the BCl_2N_3 photoproduct, has no absorption in the UV region observable in these experiments (240−450 nm), and the only photoproducts observed are those from the small amount of $BCl(N_3)_2$ that was deposited in the matrix.

Discussion

Photolysis of $B(N)_3$. The ultraviolet gas-phase absorption spectrum of $B(N_3)_3$ presented by Mulinax et al.[1] displays a strong feature at 230 nm thought to correspond to an $n \rightarrow \pi^*$ transition of the N_3 chains, causing the RN−NN bonds to rupture. Whether the three azide groups break sequentially or in a concerted fashion remains unknown; however, from the low-temperature photolysis data,[2] it is known that the linear compound NNBN is produced. The correspondence of the NNBN IR spectrum with the UV bands that appear between 345 and 380 nm leads to the assignment of these bands to NNBN.

Because NNBN is isoelectronic with C_2N_2, it is of interest to compare the electronic spectra of these molecules. There are two isomers of C_2N_2, cyanogen (NCCN) and isocyanogen (CNCN), and of these isomers, the electronic states of NCCN have been studied more extensively, both experimentally[9−11] and theoretically.[12−15] The $A^1\Sigma^-_u \leftarrow X^1\Sigma^+_g$ transition in NCCN is observed in absorption and consists of four bands. The lowest energy band is at 218.9 nm and is assigned as the 4^1_0 origin band. The NNBN UV absorption spectrum shows a series of five bands, listed in Table 1, that have an average separation of 480 cm^{-1}, a value that compares well with the calculated value of 475 cm^{-1} for ν_4 of the NNBN ground state.[2] It appears that in both NCCN and NNBN a bending mode is activated during the transition from the ground state to the lowest excited singlet

TABLE 1: UV Spectral Features of NNBN

wavelength (nm)	frequency (cm^{-1})	rel abs
348.0	28 740	0.43
353.5	28 290	0.51
360.0	27 780	0.62
366.0	27 320	0.78
372.5	26 850	1.00
379.5	26 350	0.91

state. The fact that several bands are observed for both NCCN and NNBN suggests similar relationships between the ground and excited-state potentials for the two species. The agreement between the observed band separation and ν_4 for the ground state in NNBN is an indication of the similarity of the ground- and excited-state potential surfaces along this coordinate. The 19 330 cm^{-1} energy shift between the lowest energy band observed in the NNBN progression and the 218.9 nm NCCN feature is striking and not understood at present.

The other C_2N_2 isomer, CNCN, has been deposited in a low-temperature matrix and its IR spectrum measured, following its production via thermolysis of norbornadienone azine.[16] Although there is no UV spectral data available for this compound, a computational study of its ground and first excited singlet states has been published and T_0 for the first excited singlet state is estimated to be 243 nm (41 100 cm^{-1}), shifted somewhat closer to the NNBN excited-state energy.

The 275 nm feature in the UV photolysis spectrum of the 3:1 matrix is attributed to BCl. To examine possible sources of this BCl, matrices containing BCl_3 only were prepared and photolyzed. No BCl appeared so any BCl_3 that may have been deposited at some time during the experiment cannot be its source. The source could, however, be $BCl(N_3)_2$. Even with the excess of HN_3 reactant used to prepare this matrix, small amounts of $BCl(N_3)_3$ may be deposited at some time during the deposition and serve as the BCl source. Because BCl is such a strong absorber in the UV, even small amounts are easily detected.

Photolysis of $BCl(N_3)_2$. The photolysis of $BCl(N_3)_2$ is similar to the photolysis of $B(N_3)_3$ and is assumed to involve the release of diatomic nitrogen to generate a trigonal $BClN_2$ fragment. This step is followed by rearrangement, and there are four possible rearrangement products of $BClN_2$, as shown in Figure 1C. The IR spectrum observed for the photoproduct is consistent with that calculated for the three-membered ring compound $ClBN_2$, hence the assumption that it is formed in this system. (It is noted, however, that this assignment remains tentative because only one vibrational feature and the corresponding ^{10}B isotopomer feature have been observed in the IR spectrum.) The correspondence between the appearance of the IR and UV absorption features during photolysis strongly implies that the 408 nm UV feature is due to the same photoproduct. The fact that this feature is somewhat broad with an envelope suggestive of overlapping vibrational progressions of a polyatomic species is consistent with the assignment of the 408 nm feature to the $ClBN_2$ ring compound. The decrease in the intensity of the 408 nm feature upon prolonged UV irradiation shows that the ring compound is photolytically unstable.

The other rearrangement products shown in Figure 1C are linear forms. NNBCl is not expected to be stable, and this prediction is supported by the results of geometry optimization and frequency calculations of the ground state of this species (RCISD/6-311G(D)).[17] This calculation yielded a single negative frequency along a bending mode, a motion that would ultimately lead to the formation of N_2 and BCl. The apppearance of the 275 nm peak in the UV shows the formation of BCl, and this may well be proof of the $NNBCl \rightarrow N_2 + BCl$ process, and of $N_2 + BCl$ as a second channel in the photolysis of $BCl(N_3)_2$. All photolytically stable photoproducts from a single parent must have the same formation rate, and this is clearly not the case (Figure 6). However, since the ring compound is itself photolabile, then its apparent growth should appear to be slower than that of BCl. BCl is also a likely product of the ring compound photodissociation, and this will also affect the growth of BCl.

It is clear that the appearance of BCl in the $B(N_3)_3$ photolysis system is due to the presence of $BCl(N_3)_2$ in the $B(N_3)_3$ matrix. The fact that there are only small amounts of $BCl(N_3)_2$ in the $B(N_3)_3$/Ar matrices explains why less BCl is observed than in the $BCl(N_3)_2$/Ar matrices.

The other linear forms that can result from the rearrangement of the trigonal $BClN_2$ are NBNCl or NClBN. These species are predicted by ab initio calculations (RCISD/6-311G(D)) to be unstable (not surprisingly), and dissociation to NCl + BN is expected. Upon careful examination of the IR spectra obtained during the photolysis of $BCl(N_3)_2$, peaks at 1558 and 1600 cm^{-1} with an approximately 4/1 intensity ratio and a broad weak feature in the 820−840 cm^{-1} range are detected. The 1558/1600 cm^{-1} pair could be from the B isotopomers of BN, shifted from the 1515/1567 cm^{-1} gas-phase frequencies due to matrix effects and the proximity of other species in the same matrix cage. The 820−840 cm^{-1} feature may indicate the appearance of NCl. The IR spectrum of NCl in a low-temperature argon matrix has been measured, and the reported frequencies are 817 and 824 cm^{-1} for the Cl isotopomers.[18] The possibility that all of the rearrangement channels are open for $BClN_2$ is intriguing and warrants further study.

Photolysis of BCl_2N_3. Photolysis of BCl_2N_3 produces the linear compound ClBNCl, a molecule that is isoelectronic with dichloroacetylene. In a low-temperature matrix study of the $ClCCCl^+$ cation, Leutwyler et al. deposited ClCCCl in a neon matrix and reported that there were no absorption features at wavelengths longer than 280 nm for this molecule.[19] More detailed information regarding the absorption spectrum of dichloroacetylene is not available, so comparisons to ClBNCl is difficult. However, it is clear that for ClBNCl, there is no absorption at wavelengths longer than 240 nm.

The UV spectrum does show that BCl is generated as the photolysis proceeds. The source of this BCl cannot be ClBNCl since this compound is photolytically stable. Even upon prolonged UV photolysis, no decreases in its IR spectrum are observed. No evidence of other photoproducts from the photolysis of BCl_2N_3 has been detected in the IR spectra that might form from other rearrangement processes of the initially formed trigonal $BClN_2$. Consequently, it is assumed that the BCl is from small amounts of $BCl(N_3)_2$ deposited in the matrix as is the case in the $B(N_3)_3$ system. The very weak feature at 408 nm supports this assumption.

Conclusion

The goal of the research reported here was to measure the UV absorption spectra for the intermediates generated during photolysis of $B(N_3)_3$, $BCl(N_3)_2$, and BCl_2N_3 isolated in low-temperature argon matrices. The intermediate produced in the $B(N_3)_3$ photolysis was identified as NNBN on the basis of its IR spectrum, ab initio calculations, and isomer shifts. The assignment of the band system in the UV between 345 and 380 nm to NNBN is based on fact that these bands appear at the same rate as the NNBN IR features as the photolysis proceeds. This is very strong support for the assignment, but not definitive. The assignment of the band system to a vibrational progression

in a bending mode of NNBN is therefore somewhat tentative. Adding to the strength of this assignment, the recorded UV spectrum is similar to what is observed in the isoelectronic molecule NCCN.

When $BCl(N_3)_2$, isolated in a low-temperature argon matrix is photolyzed, the IR spectrum showed two features at 1677 and 1724 cm^{-1} and the UV spectrum showed a broad feature at 408 nm. The IR and UV features appeared at the same rate as the photolysis proceeded, and upon extended photolysis, decayed. The IR features have been tentatively identified as the three-membered ring compound, $ClBN_2$, so the UV feature at 408 nm is likewise assigned. Now that the absorption spectrum of the intermediate generated via photolysis of $BCl(N_3)_2$ is known, LIF studies are planned.

The compound produced from the photolysis of BCl_2N_3 is known to be the linear molecule ClBNCl; however, unlike the other two systems, no UV absorption spectrum was detected for this molecule.

Since NCCN emits upon excitation of its lowest excited singlet state, there is a good probability that NNBN will also. Consequently, laser-induced fluorescence studies on NNBN first in the low-temperature matrix and then in gas-phase systems are planned. With knowledge of the absorption spectrum of NNBN, fluorescence experiments can be carried out to learn more about the electronic structure of this molecule. In addition, fluorescence will be a very useful probe for detecting the presence of NNBN in various $B(N_3)_3$ decomposition systems. If NNBN is key to film formation, then it will be observed when the decomposition conditions are appropriate for BN film production. Additional spectral information on the intermediate generated from $BCl(N_3)_2$, identified as the ring species $ClBN_2$ is also being sought. Finally, these studies will be extended to included Al-azide and Ga-azide systems.

Acknowledgment. This work was supported by the National Science Foundation under grant CHE-9527080.

References and Notes

(1) Mulinax, R. L.; Okin, G. S.; Coombe, R. D. *J. Phys. Chem.* **1995**, *99*, 6294.

(2) Al-Jihad, I. A.; Liu, B.; Linnen, C. J.; Gilbert, J. V. *J. Phys. Chem.* **1998**, *102*, 6220.

(3) Andrews, L.; Hassanzadeh, P.; Burkholder, T. R.; Martin, J. M. L. *J. Chem. Phys.* **1993**, 9*8*, 922.

(4) Johnson, L. A.; Sturgis, S. A.; Al-Jihad, I. A.; Liu, B.; Gilbert, J. V. *J. Phys. Chem. A* **1999**, *103*, 686.

(5) Travers, M. J.; Eldenburg, E. L.; Gilbert, J. V. *J. Phys. Chem. A* **1999**, *103*, 9661.

(6) Paetzhold, P. I.; Gayoso, M.; Dehnicke, K.; Z. Chem. Ber. **1965,** *98*, 1173.

(7) Schlie, L. A.; Wright, M. W. *J. Chem. Phys*. **1990**, *92*, 394.

(8) Pearse, R. W. B.; Gaydon, A. G. *The Identification of Molecular Spectra*, 4th ed.; Chapman & Hall: New York, 1976.

(9) Barts, S. A.; Halpern, J. B. *Chem. Phys. Lett.* **1989**, *161*, 207.

(10) Connors, R. E.; Roebber, J. L.; Weiss, K. *J. Chem. Phys.* **1974**, *60*, 5011.

(11) Wannenmacher, E. A. J.; Lin, H.; Jackson, W. M. *J. Phys. Chem.* **1990**, *94*, 6608.

(12) Bell, S. *Chem. Phys. Lett.* **1979**, *67*, 498.

(13) Dateo, C. E.; Dupuis, M.; Lester, W. A., Jr. *J. Chem. Phys.* **1985**, *83*, 265.

(14) Botschwina, P.; Sebald, P. *Chem. Phys.* **1990**, *141*, 311.

(15) Botschwina, P.; Flügge, J. *Chem. Phys. Lett.* **1991**, *180*, 589.

(16) Stroh, F.; Winnewisser, B. P.; Winnewisser, M.; Reisenauer, H. P.; Maier, G.; Goede, S. J.; Bickelhaupt, F. *Chem. Phys. Lett.* **1989**, *160*, 105.

(17) Frisch, M. J.; Trucks, G. W.; Schlegel, H. B.; Gill, P. M. W.; Johnson, B. G.; Robb, M. A.; Cheeseman, J. R.; Keith, T.; Petersson, G. A.; Montgomery, J. A.; Raghavachari, K.; Al-Laham, M. A.; Zakrzewski, V. G.; Ortiz, J. V.; Foresman, J. B.; Cioslowski, J.; Stefanov, B. B.; Nanayakkara, A.; Challacombe, M.; Peng, C. Y.; Ayala, P. Y.; Chen, W.; Wong, M. W.; Andres, J. L.; Replogle, E. S.; Gomperts, R.; Martin, R. L.; Fox, D. J.; Binkley, J. S.; Defrees, D. J.; Baker, J.; Stewart, J. P.; Head-Gordon, M.; Gonzalez, C.; Pople, J. A. *Gaussian 94*, Revision E.2; Gaussian, Inc.: Pittsburgh, PA, 1995.

(18) Milligan, D. E.; Jacox, M. E. *J. Chem. Phys.* **1964**, *40*, 2461.

(19) Leutwyler, S.; Maier, J. P.; Spittel, U. *Mol. Phys.* **1984**, *51*, 437.